ACS OMEGA

http://pubs.acs.org/journal/acsodf

Article

Experimental and Kinetic Study of the Effect of Nitrogen Dioxide on Ethanol Autoignition

Yifan Jin, Zhihao Ma,* Xin Wang, Fangjie Liu, Xin Li, and Xianglin Chu

Cite This: *ACS Omega* 2023, 8, 8377−8387

Read Online

ACCESS | Metrics & More | Article Recommendations | Supporting Information

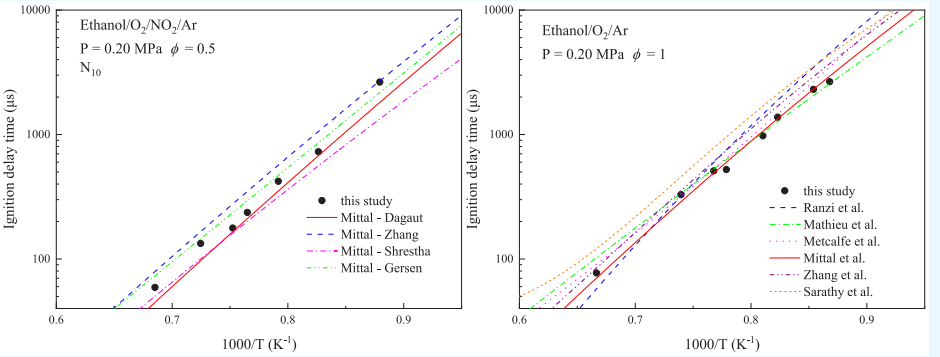

ABSTRACT: The contribution of NO_2 to the ethanol ignition delay time was investigated behind reflected shock waves. The experiments were performed at a pressure of 0.20 MPa, temperature range of 1050−1650 K, equivalence ratio of 0.5/1.0/1.5, and ethanol/NO_2 mixing ratios of 100/0, 90/10, and 50/50. The experimental results showed that the addition of NO_2 decreased the ignition delay time and promoted the reactivity of ethanol under all equivalence ratios. With an increase in NO_2 blending, the effect of equivalence ratio on the ethanol ignition delay time decreased, and with an increase in temperature, the effect of NO_2 in promoting ethanol ignition weakened. An updated mechanism was proposed to quantify NO_2-promoted ethanol ignition. The mechanism was validated based on available experimental data, and the results were in line with the experimental trends under all conditions. Chemical kinetic analyses were performed to interpret the interactions between NO_2 and ethanol for fuel ignition. The numerical analysis indicated that the promotion effect of NO_2 is primarily due to an increase of the rate of production and concentration of the radical pool, especially the OH radical pool. The reaction NO + HO_2 ⇔ NO_2 + OH is key to generating chain-initiating OH radicals.

1. INTRODUCTION

Ethanol is a clean renewable fuel, and blending it with conventional fuels can help reduce the potential engine knock while improving the fuel economy.[1] The use of ethanol directly or as a gasoline additive can considerably reduce CO and HC emissions.[2,3] In addition, ethanol combustion has a faster flame speed, which helps to increase the combustion rate of the mixture inside the engine cylinder. However, ethanol combustion still results in a considerable generation of nitrogen oxides (NO_X). Exhaust gas recirculation (EGR) can significantly reduce NO_X emissions in combustion engines. NO in EGR gas is readily interconverted to NO_2 because of the dilution and oxidation of fresh intake air.[4−6] Research has shown that low amounts of NO_X promote hydrocarbon combustion and ignition delay times.[7,8] Thus, to evaluate the effect of NO_X on ethanol combustion, it is crucial to establish a well-validated kinetic model for ethanol/NO_X.

Several studies have investigated the chemical kinetics of the ignition and combustion of ethanol. These include combustion engines,[9,10] shock tubes,[11−13] rapid compression machines (RCMs),[14,15] flow reactors,[16] and jet-stirred reactors.[17] Laich et al.[18] measured the ignition delay time and CO time histories for ethanol based on a shock tube at the pressure of 17.8−23.9 atm and the temperature range of 960−1580 K. The experimental analysis concluded that early heat release led to preignition, illustrating the pathways of ethanol formation and decomposition. Nativel et al.[19] investigated the ignition delay of ethanol with different levels of inert gas dilution at stoichiometric equivalence ratios at 20 atm and a test temperature range of 800−1250 K in a shock tube. They observed temporal and spatial differences in the ignition modes under different conditions. In addition, different degrees of nonhomogeneous preignition in the low-temperature range of

Received: November 7, 2022
Accepted: February 13, 2023
Published: February 22, 2023

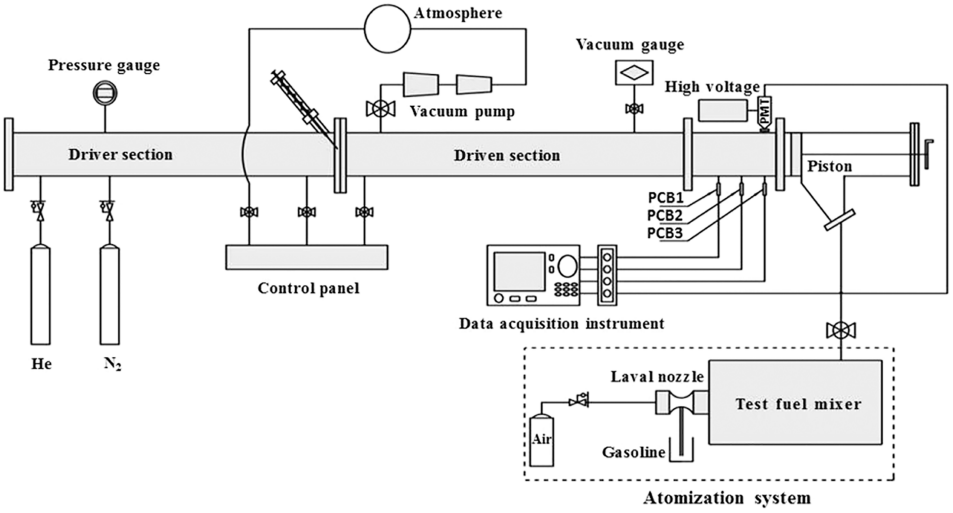

Figure 1. Schematic diagram of the shock tube apparatus.

800−860 K were observed using high-repetition-rate color imaging cameras. They found that the addition of a low concentration of helium to the mixture was very effective in suppressing preignition as it changes the high heat release and low thermal diffusivity, thus suppressing the formation of local temperature inhomogeneities. Barraza-Botet et al.[14] conducted an investigation on the ignition delay time for ethanol in the temperature range of 800−1150 K and pressure range of 3−10 atm in RCM. It was found that the interaction reaction between ethanol and HO_2 is important for the ignition delay times and for accurate updating of the rate coefficients for this reaction. Cheng et al.[20] investigated the ignition delay of ethanol in a RCM at pressure of 19.7−39.4 atm and the temperature range of 780−950 K. They found that the most important promoting reaction for ethanol is the H atom abstraction by HO_2.

Recently, many researchers have investigated the kinetic effects of NO_2 on the combustion characteristics of hydrocarbon fuels. Sahu et al.[21] investigated the ignition delay time of CH_4 in a RCM and in a shock tube at temperature range of 900−1500 K, pressure range of 14.8−29.6 atm, and equivalence ratios of 0.5−2.0. They found that the addition of 200 ppm NO_2 to the CH_4/O_2 mixture with equivalence ratio of 1.0 in the temperatures of 600−1000 K results in a 3-fold increase in reactivity compared to the case without NO_2. Mohamed et al.[22] investigated the ignition delay times of ethane in a RCM at pressure of 19.7−29.6 atm and the temperature range of 851−1390 K. They found that the addition of 1000 ppm NO_2 significantly promotes the reactivity of ethane/air mixtures. Deng et al.[23] investigated the effect of NO_2 addition on the ignition delay time of ethylene and proposed an ethylene/NO_2 model using a shock tube. They found that the promotion of ethylene by NO_2 was strongly dependent on the pressure, temperature, and equivalence ratio. They concluded that NO_2, owing to its high reactivity, could increase the system reactivity by directly reacting with the fuel and increasing the consumption rate of intermediates such as CH_3 and CH_2O. Wu et al.[24] investigated the ignition delay times of n-C_4H_{10} at the temperature range of 700−1200 K, the pressure of 19.7 atm, and equivalence ratios from 1.0 to 2.0. The results showed that the effect of NO_2 on the ignition of n-C_4H_{10} exhibited temperature and NO_2 concentration dependence.

Shi et al.[25] studied the effect of the addition of small amounts of NO_2 on the ignition delay time of n-heptane in a shock tube and proposed a n-heptane/NO_2 kinetic model. The results showed that NO_2 blending significantly reduced the ignition delay time. When the temperature was higher than 860 K, the promotion effect of NO_2 was enhanced with the increase in NO_2 concentration, but with the temperature lower than 860 K, the incorporation of 1% NO_2 had less promotion effect than 0.5%, and with NO_2 blending, the effect of the ignition delay time of n-heptane at approximately 700 K was minimal. This is because $C_7H_{15} + NO_2 \Leftrightarrow C_7H_{15}O + NO$ and $NO_2 + OH\ (+M) \Leftrightarrow HNO_3\ (+M)$ have a strong inhibiting influence on the ignition of n-heptane, which weakened the NO_2 ignition in the low-temperature region. Ye et al.[26] studied the effects of different NO_2 concentrations of the ignition characteristics on DME using a shock tube. The results showed that the effect of NO_2 promoting on DME ignition was evident, and it enhanced with the increase in NO_2 concentration. NO_2 promoting effect was stronger at lower temperatures than that at higher temperatures. Kinetic mechanism analysis showed that NO_2 promoting effect on DME combustion was mostly as a result of the generation of a significant amount of OH and H radicals through the interconversion of NO and NO_2, which in turn promotes reactivity of the reaction system. Moreover, many scholars have conducted similar studies, and the results indicate that the blending of NO_2 and other NO_X in the fuel has a certain promotion effect on the oxidation of the fuel.[27−29]

However, the kinetic mechanisms of ethanol/NO_X are still underexplored. Yang et al.[30] investigated the influence of NO on the ignition delay of n-heptane/ethanol fuel mixtures with equivalence ratios of 0.5, 1, and 1.5, a temperature range of 900−1200 K, and a pressure of 10 atm in a shock tube. Alzueta and Hernández[31] investigated the ethanol/NO model in an isothermal quartz flow reactor at a pressure of 1 atm, in the temperature range 700−1500 K. The effects of NO on the concentrations of ethanol, CO, and CO_2 were analyzed. The results showed that the influence of NO on ethanol oxidation changed with equivalence ratio. When the equivalence ratio decreases, ethanol oxidation at lower temperatures is promoted, but NO inhibits ethanol consumption at rich equivalence ratio. They suggested that the cycle between NO and NO_2 is the principle of NO_2 promotion of fuel ignition,

https://doi.org/10.1021/acsomega.2c07167
ACS Omega 2023, 8, 8377−8387

where NO_2 promotes fuel consumption and converts HO_2 radicals to the more important chain-initiating OH radicals, in agreement with Deng et al.[23] and Ye et al.[26]

To the best of our knowledge, there is a lack of kinetic studies on the ignition behavior of NO_2 addition to ethanol. The objective of this study is to investigate the promoting principle of NO_2 on ethanol combustion. The ignition delay times were measured in a shock tube, and the temperature dependence of NO_2 on the ignition delay times of ethanol was investigated. Furthermore, a kinetic mechanism for ethanol/NO_2 mixtures is proposed and validated using experimental results. Sensitivity and pathway analyses were conducted to explain the effect of NO_2 on ethanol ignition.

2. EXPERIMENTAL SETUP

2.1. Experimental Method. The experiments were performed in a stainless-steel chemical shock tube with an inner diameter of 100 mm and a wall thickness of 17.5 mm. The tube consisted of a 4.0 m long driver section and a 5.5 m long driven section. In the middle, polycarbonate diaphragms were punctured using a needle-punched diaphragm-breaking mechanism to satisfy the test requirements under different conditions. The test setup is shown in Figure 1, where fast-response piezoelectric pressure transducers (PCB113B24) were installed at the end of the driven section, PCB3 was located 20 mm from the end wall, and the distance between each pressure transducer was 200 mm to measure the velocity of the incident shock wave. A photoelectric multiplier (PMT, Hamamatsu CR131) mounted in the same axial position as the PCB3 pressure transducers and a 307 ± 7.5 nm bandpass filter located at the front of the PMT were used to record the OH radical emissions. The function of the piston device with large diameter and low flow rate is to introduce a homogeneous mixture into the shock tube.

To prevent possible condensation of ethanol, the partial pressure of ethanol in the mixing tank was maintained below 50% of its saturated vapor pressure. The driven section and mixing tank were heated to 353 K, using a heating jacket, which was above the boiling point of ethanol and allowed ethanol to evaporate completely. The mixture was premixed for 12 h to ensure homogeneity and complete vaporization. Before the experiment, the shock tube was evacuated to a pressure below 5 Pa using a vacuum pump and the experimental mixture was prepared according to Dalton's law of partial pressure. All of the gases used were high purity (99.9% purity for C_2H_5OH, 99.999% purity for O_2, 99.999% purity for Ar, 99.99% purity for NO_2, and 99.99% purity for He). The molar compositions of the mixtures are listed in Table 1.

Table 1. Compositions of the Experimental Gas Mixture

Mixture	ϕ	P/MPa	C_2H_5OH/%	O_2/%	Ar/%	NO_2/%
1	0.5	0.2	2.0	12.0	86.0	0
2	0.5	0.2	2.0	12.0	85.8	0.2
3	0.5	0.2	2.0	12.0	85.0	1.0
4	1.0	0.2	2.0	6.0	92.0	0
5	1.0	0.2	2.0	6.0	91.8	0.2
6	1.0	0.2	2.0	6.0	91.0	1.0
7	1.5	0.2	2.0	4.0	94.0	0
8	1.5	0.2	2.0	4.0	93.8	0.2
9	1.5	0.2	2.0	4.0	93.0	1.0

The ignition delay time used in this study was determined as the interval between the reflected shock arrival detected using the PCB3 pressure transducers near the end wall and the greatest slope of the OH* chemiluminescence emission signal to its zero level on the time axis, as shown in the Figure 2. The

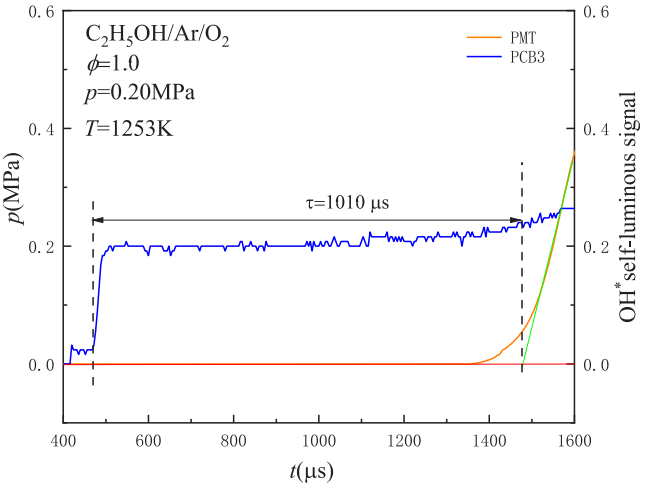

Figure 2. Definition of typical shock tube ignition delay time.

reflected shock temperature and pressure were calculated using Gaseq,[32] which is a software for chemical equilibrium according to the reflected shock wave speed. The standard square root (RSS) method[33] was used to assess the uncertainty,

$$T_S = \frac{T_1[2(\gamma-1)M^2+(3-\gamma)][(3\gamma-1)M^2-2(\gamma-1)]}{(\gamma+1)^2M^2} = AM^2 + B + CM^{-2} \quad (1)$$

$$M = \frac{V_S}{\sqrt{\gamma R T_1}} \quad (2)$$

$$\delta V_S = \sqrt{\left(\frac{1}{\Delta t}\delta_{\Delta z}\right)^2 + \left(\frac{-\Delta z}{\Delta t^2}\delta_{\Delta t}\right)^2} \quad (3)$$

$$\delta T_S = \frac{\partial^2 T_S}{\partial M}\delta M = (2AM - 2CM^{-3})\frac{\delta V_S}{\sqrt{\gamma_1 R T_1}} \quad (4)$$

where T_S is the reflected shock temperature (K); T_1 is the initial temperature (K); γ is the adiabatic exponent; V_S is the velocity of the incident shock wave (m/s); and R is the universal gas constant. The main source of measurement uncertainty is T_S, which is estimated to be no more than 20 K using eqs 1−4, leading to a maximum uncertainty in ignition delay times within ±18%, depending on the experimental conditions.

2.2. Kinetic Mechanism. CHEMKIN Pro[34] was used to determine kinetic analysis of combustible gas mixtures in a constant volume homogeneous reaction system. The ethanol models of Zhang et al.,[13] Ranzi et al.,[35] Mathieu et al.,[36] Metcalfe et al.,[37] Sarathy et al.,[38] and Mittal et al.[15] were chosen to evaluate their performance against the measured ignition delay time. From Figure 3, all of the models above reproduce the experimental data well under the experimental conditions. The model developed by Mittal et al.[15] was chosen as the ethanol kinetic submodel, which complements the

https://doi.org/10.1021/acsomega.2c07167
ACS Omega 2023, 8, 8377−8387

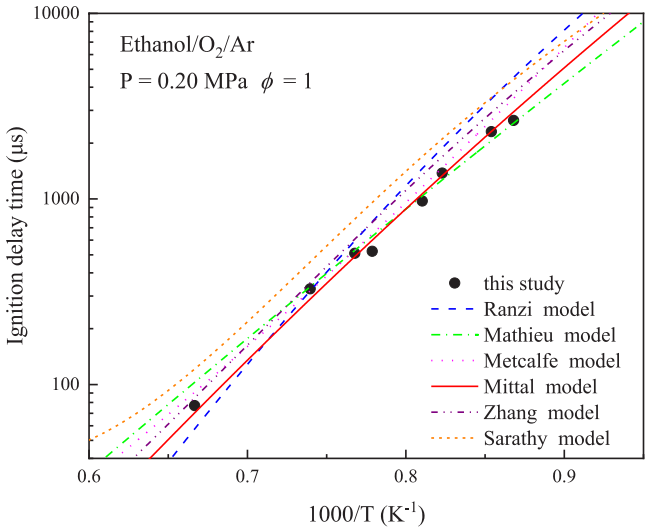

Figure 3. Comparison between the measured data and the predictions with four models for $C_2H_5OH/O_2/Ar$ mixture (ϕ = 1.0; P = 0.20 MPa). Symbols represent experimental measurements in this study. Lines denote the model-predicted ignition delay times using different models.

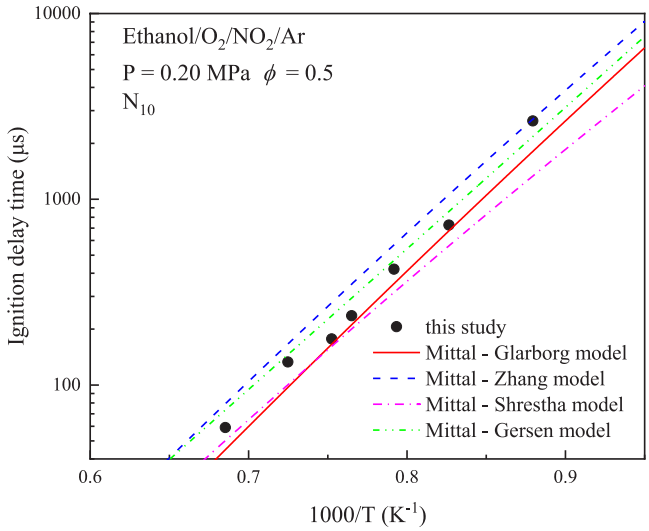

Figure 4. Comparison between the measured data and the predictions with four assembled models for N_{10} mixture (ϕ = 0.5; P = 0.20 MPa). Symbols represent experimental measurements in this study. Lines denote the model-predicted ignition delay times using different assembled models.

experimental data of ethanol at low and medium temperatures and a wide pressure range, which fits well with the data of ethanol ignition delay time measured in this study. The mechanism is validated by the experimental data of various basic combustion equipment, which have a high calculation accuracy and wide application range.

For NO_X chemistry, four literature models were selected: Zhang et al.,[39] Shrestha et al.,[40] Gersen et al.[28] and Glarborg et al.;[41] these models all contain a complete NO_X submodel. Among them, the NO_X submodel of Zhang et al.[39] is based on the study of Bugler et al.,[42] and all of the kinetic parameters for HON related reactions are adopted from the recommendations of Dean and Bozzelli.[43] The model of Shrestha et al.[40] is based on Baulch et al.[44] and was optimized with experimental data from the literature, and C2 and NO_X-related chemical reactions were added. Gersen et al.[28] developed it based on the study of Rasmussen et al.,[45] and the rate constants of the reaction $CH_4 + NO_2 \Leftrightarrow CH_3 + HONO$ was taken from Dean et al.[43] Glarborg et al.'s[41] model is based on the work of Klippenstein et al.,[46] with an update for selecting the key reactions. For the purpose of making a better comparison of the NO_X models, the NO_X models in the above four literature citations were combined with Mittal et al.'s[15] model for reducing the influence of the hydrocarbon submodel. Herein, the combined models are called the Mittal−Zhang model, the Mittal−Shrestha model, the Mittal−Gersen model, and the Mittal−Glarborg model, respectively. The measured ignition delay times are compared with the assembled models, as shown in Figure 4. Compared to experimental data, the Mittal−Glarborg model exhibited better agreement. Therefore, the Mittal−Glarborg model was chosen as the base model for ethanol/NO_2 mixtures. However, Mittal et al.[15] pointed out the consistent underprediction of ethylene concentrations across a range of conditions. Therefore, the reactions $PC_2H_4OH + H \Leftrightarrow C_2H_4 + H_2O$ and $C_2H_4 + NO_2 \Leftrightarrow C_2H_3 + HONO$ from the study of Deng et al.[23] were added. And Zhang et al.'s[39] rate constant was adopted for the reaction $C_2H_5OH + HO_2 \Leftrightarrow CH_3CHOH + H_2O_2$.The updated mechanism obtains a better simulation agreement against our experimental data. The added reactions and rate coefficients were tabulated in Table 2.

3. RESULTS AND DISCUSSION

3.1. Effect of Equivalence Ratios. Figure 5 illustrates the ignition delay times for ethanol/NO_2/O_2/Ar mixtures at different equivalence ratios. N_0, N_{10}, and N_{50} indicate the NO_2 blending amounts of 0%, 10%, and 50% of the fuel, respectively. At higher temperature, the ignition delay time increases with equivalence ratio increasing, whereas the ignition delay time varies slightly with equivalence ratio at lower temperature. The crossover of the ignition delay time curves was observed for the N_{50} mixture in the low-temperature region for different equivalence ratios. Figure 6 presents the ignition delay time reduction rates for different equivalence ratios of the N_{10} and N_{50} mixtures compared to N_0 at 0.20 MPa. In more detail, at 1150 K, 1.5, 1.0, and 0.5 equivalence ratios reduce ignition delay time by about 42.8%, 38.2%, and 28.9% in N_{10} mixture and by about 67.8%, 60.9%, and 51.9% in N_{50} mixture.

3.2. Effect of NO_2 Blending. Figure 7 illustrates the ignition delay times for ethanol/NO_2/O_2/Ar mixtures under different NO_2 proportions. Under similar equivalence ratios, the addition of NO_2 to the fuel can reduce the ignition delay time of ethanol significantly and promote ignition effectively. As shown in Figure 6, at 1450 K, blending 10% NO_2 resulted in a 16.5% reduction in ignition delay time compared to the neat mixture, and blending 50% NO_2 resulted in a 40.2% reduction. For the lean fuel condition, 18.3% and 50.5% reductions were observed on blending with 10% and 50% NO_2, respectively. For the rich fuel condition, 11.1% and 23.6% reductions were observed when 10% and 50% NO_2 were added to the mixture, respectively. In general, with the addition of NO_2, the reduction in ignition delay time increased with increasing equivalence ratio. The ignition delay times decrease significantly with increasing NO_2 concentration, and this decrease becomes moderate with increasing NO_2 concentration.

https://doi.org/10.1021/acsomega.2c07167
ACS Omega 2023, 8, 8377−8387

Table 2. Selected Reactions in the Developed Mechanism[a]

Reaction	A	n	E_a	Source
$C_2H_5OH + HO_2 \Leftrightarrow PC_2H_4OH + H_2O_2$	2.1×10^{-5}	5.260	6500	13
$PC_2H_4OH + H \Leftrightarrow C_2H_4 + H_2O$	3.6×10^{16}	−0.716	8766	23
$C_2H_4 + NO_2 \Leftrightarrow C_2H_3 + HONO$	31.69	3.765	31816	23
$C_2H_4 + NO_2 \Leftrightarrow C_2H_3 + HNO_2$	485.38	3.178	34686	23

[a]Rate constants, $k = AT^n \exp(E_a/(RT))$, are expressed in units of cm^3, mol^{-1}, s^{-1}, and cal.

3.3. Mechanism Analyses. *3.3.1. Sensitivity Analysis.* The previous analysis demonstrated that NO_2 significantly promotes the ignition of ethanol, and at low temperatures, the promotion effect was especially evident. Therefore, to identify the essential reactions involving radicals of the dominant ethanol ignition under NO_2 blending conditions, a sensitivity analysis of the ignition delay time was performed at P = 0.20 MPa, T = 1150 K, and stoichiometric condition. 1150 K is close to the minimum temperature for this test, and the effect of NO_2 on the fuel ignition delay time is particularly pronounced at low temperatures. The sensitivity coefficient was defined as follows:

$$S_i = \frac{\tau(2k_i) - \tau(0.5k_i)}{1.5\tau(k_i)} \quad (5)$$

where τ is the ignition delay time, S_i is the sensitivity coefficient of the elementary reaction to the ignition delay time, and k_i is the reaction rate coefficient of the ith elementary reaction.

Figure 8 shows the sensitivity analysis of ethanol with different NO_2 blending ratios. For the N_0 mixture, the most sensitive reaction was R368 ($C_2H_5OH + HO_2 \Leftrightarrow SC_2H_4OH + H_2O_2$). This is because R368 and R16 ($HO_2 + HO_2 \Leftrightarrow H_2O_2 + O_2$) were the main sources of H_2O_2 in the reaction system. Once H_2O_2 is formed, it immediately decomposes into OH radicals through R19 ($H_2O_2(+M) \Leftrightarrow OH + OH(+M)$). The formed SC_2H_4OH continues to react with O_2 to produce CH_3CHO and HO_2, and the generated HO_2 radicals are involved in reactions R369 ($C_2H_5OH + HO_2 \Leftrightarrow PC_2H_4OH + H_2O_2$), R251 ($CH_3CHO + HO_2 \Leftrightarrow CH_3CO + H_2O_2$), and R144 ($CH_3 + HO_2 \Leftrightarrow CH_3O + OH$). Moreover, the generated HO_2 radicals further promoted reaction R368, further promoting ignition. In addition, the promotion of ignition by R1 ($H + O_2 \Leftrightarrow O + OH$) is also evident as R1 is also the first chain reaction that promotes ignition in most hydrocarbon fuels, as it generates more reactive O and OH radicals, thus promoting reactivity. Among the ignition inhibition reactions, the termination reaction R145 ($CH_3 + HO_2 \Leftrightarrow CH_4 + O_2$) is the most sensitive. The CH_3 radicals in reaction R145 are mainly generated by the decomposition of CH_3CO, while stable species of CH_4 and O_2 are produced, thus inhibiting the reactivity. Similarly, the other termination reactions, R16 ($HO_2 + HO_2 \Leftrightarrow H_2O_2 + O_2$), R245 ($CH_3CHO + H \Leftrightarrow CH_3CO + H_2$), and R14 ($HO_2 + OH \Leftrightarrow H_2O + O_2$), are due to the generation of stable species of H_2 or H_2O by consuming radicals like HO_2, OH, and H.

Some of the radical reactions involving NO_X showed greater promotion of ethanol ignition in the presence of NO_2. From Figure 8b, compared with the N_0 mixture, in the N_{10} and N_{50} mixtures, the reaction with the most was still R368, indicating that the presence of NO_2 did not replace the reaction with the promoting effect, and the sensitivity coefficient of R368 increased as the NO_2 concentration increased. In addition, with the addition of NO_2, the NO_2-relevant reactions become increasingly important. As NO_2 increases, the sensitivity coefficient of reaction R805 ($NO + HO_2 \Leftrightarrow NO_2 + OH$) becomes larger. R805 generates a large number of OH radicals via mutual sensitization oxidation of NO and NO_2. R937 ($CH_3 + NO_2 \Leftrightarrow CH_3O + NO$) is another reactivity-promoting reaction that occurs in the presence of NO_2. This is because R937 consumes methyl radicals and produces NO through a reaction with NO_2, while the formed NO can react with R805 to produce OH radicals, and converts CH_3 radicals into reactive CH_3O radicals, increasing the system reactivity.

Compared to the N_0 mixture, R14 ($HO_2 + OH \Leftrightarrow H_2O + O_2$) replaced R145 as the strongest reaction inhibiting ignition in the presence of NO_2. This is because the addition of NO_2 leads to a strong growth in the OH radical pool concentration, thus promoting the reactivity of OH-related reactions. Notably, the sensitivity coefficients of the four reactions with the most significant reactions inhibiting ignition in both the N_{10} and N_{50} mixtures decreased relative to those in the N_0 mixture. The effect of NO_2 on ignition inhibiting reactions increases with increasing NO_2 concentration.

It can be seen that NO_2 increases the concentration of the radical pool, thus promoting the consumption of important intermediate species during ethanol combustion. This includes an increase in the concentration of radicals that promote reactions, such as H_2O and OH. However, owing to the high reactivity of NO_2, some reactive intermediate species are generated during the reaction, leading to further reactions of relatively unreactive species such as CH_3. For example, R145, as the maximum sensitivity coefficient in the absence of NO_2, hinders further reactions. However, in the presence of NO_2, the consumption rate of CH_3 increased with the NO_2 blending ratio increasing, which led to a decrease in the sensitivity coefficient of R145, thus increasing the reactivity of the system.

3.3.2. Reaction Pathway. Kinetic analyses were performed using a kinetic mechanism to further understand the reasons for promoting ignition. The reaction pathway at T = 1150 K and P = 0.20 MPa of stoichiometric ethanol/NO_2 blends is given in Figure 9 at 20% ethanol consumption. For the N_0 mixture, the consumption of ethanol mainly through the H atom abstraction reactions initiated by O, H, OH, HO_2, and CH_3. Among the various small-molecule radicals, the H atom abstraction reactions initiated by OH radicals accounted for 59.71% of the total consumption ratio of ethanol, and the contribution of H atom abstraction reactions initiated by other small-molecule radicals to the total consumption ratio of ethanol was approximately 35%. The other consumption pathway of ethanol is the single-molecule dissociation reaction triggered by the breakage of C−C and C−O bonds to generate CH_3 and CH_2OH radicals, which account for approximately 5% of the total consumption of ethanol. The interaction of CH_2OH radicals from ethanol decomposition with O_2 is one of the important pathways to generate HO_2 radicals. The generated HO_2 radicals further react with ethanol to form SC_2H_4OH, which also has the largest sensitivity factor. The

https://doi.org/10.1021/acsomega.2c07167
ACS Omega 2023, 8, 8377−8387

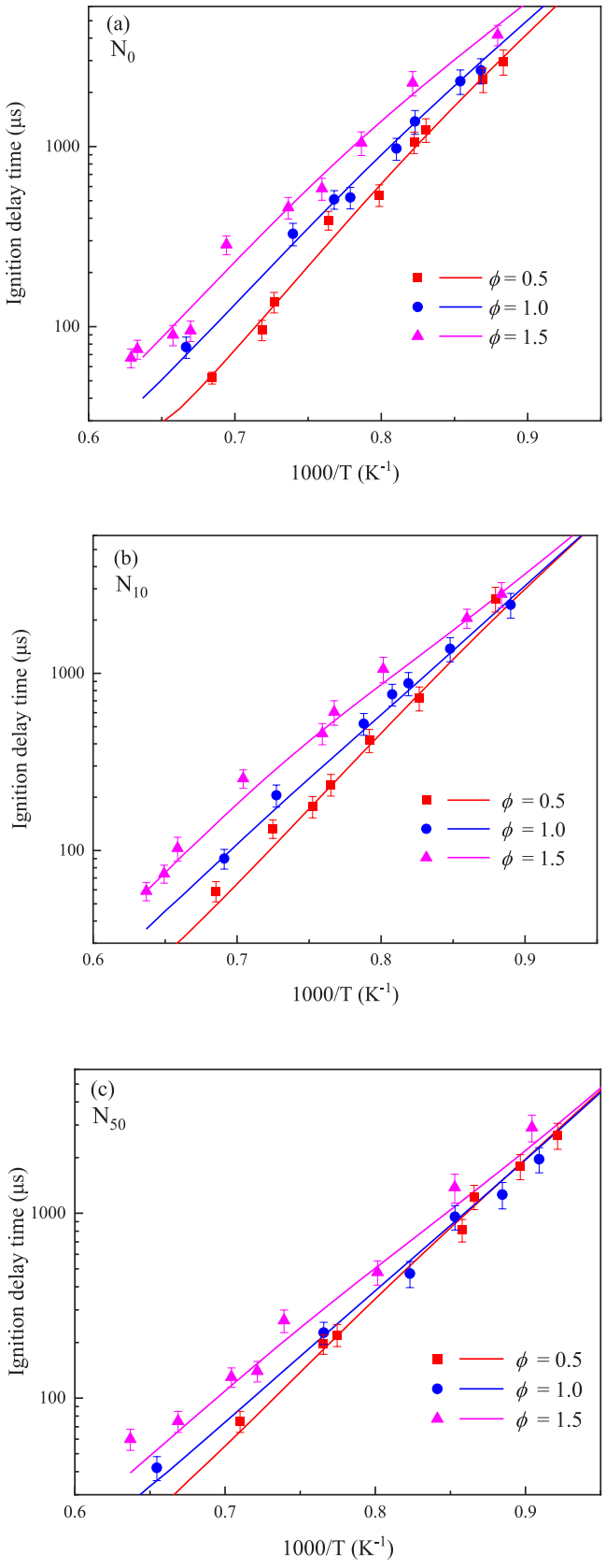

Figure 5. Ignition delay of $C_2H_5OH/NO_2/O_2/Ar$ mixtures with different equivalent ratios: (a) N_0, (b) N_{10}, and (c) N_{50}.

generated SC_2H_4OH further generates acetaldehyde (CH_3CHO) through reaction with O_2 or the H-abstraction

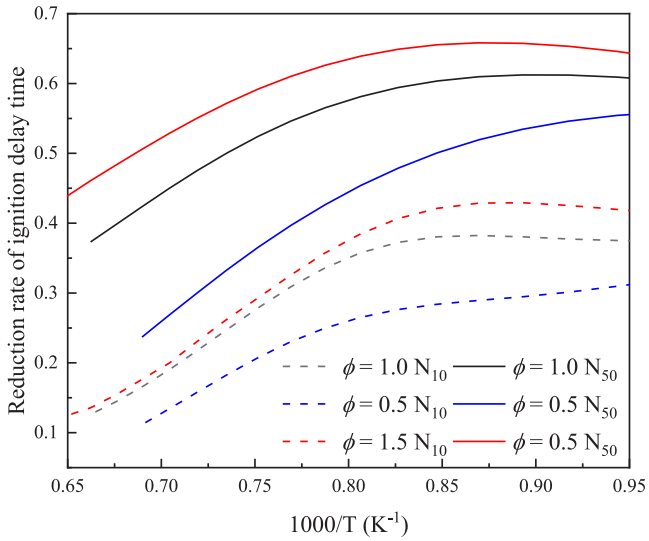

Figure 6. Reduction rate of ignition delay time.

reaction, and CH_3CHO undergoes the H atom abstraction reaction initiated by OH and H radicals to generate CH_3CO and subsequent β-scission reactions that produce CO and CH_3 radicals. Ethanol also generates ethylene through thermal dehydration. Most of them and PC_2H_4OH undergo the β-scission reaction to generate C_2H_4. The C−H bond in the intermediate position of ethanol is broken to generate vinyl alcohol (C_2H_3OH). This generates C_2H_3 owing to the interaction of C_2H_4 with H and OH radicals, followed by a series of oxidation reactions to generate the final products, CO and CO_2.

According to the simulation results, the addition of 10% NO_2 significantly shortened the ethanol ignition delay time; however, the ethanol consumption pathway did not change significantly. A slight addition of NO_2 increases the concentration of the O/OH radical pool. leading to a significant expansion of the branching ratios of the ethanol consumption reaction through OH radical-initiated H atom abstraction. From the previously described sensitivity analysis, reaction R805 associated with NO_X greatly contributes to the production of OH radicals. With a further increase in the NO_2 proportion, the influence of NO_2 kinetics on the entire reaction pathway became more evident and the relevant reaction branch ratio of NO_2 expanded significantly.

In contrast, the contribution of radicals other than OH to ethanol consumption decreased significantly. Additionally, the O−H bond, which has the highest bond energy in ethanol, also breaks and reacts with OH radicals to form C_2H_5O in the N_{10} and N_{50} mixtures because of the increased activity within the system. The H atom abstraction reaction of the OH radicals in the N_0 mixture occurs only in the C−H bond with a lower bond energy, which is a new reaction pathway for ethanol that is not observed in the N_0 mixture. Among the intermediates in ethanol oxidation, CH_2CHO is directly related to NO_X. For N_0 mixtures, the intermediate product CH_2CHO is consumed through the decomposition reaction, whereas the intermediate product CH_2CO is produced, and the subsequent decomposition produces CO or generates CO directly. For the N_{10} and N_{50} mixtures, the intermediate product CH_2CHO can directly react with NO_2 to form CH_2CO and HONO. HONO rapidly decomposes into OH radicals and NO, and NO further increases the amount of OH radicals generated through the

https://doi.org/10.1021/acsomega.2c07167
ACS Omega 2023, 8, 8377−8387

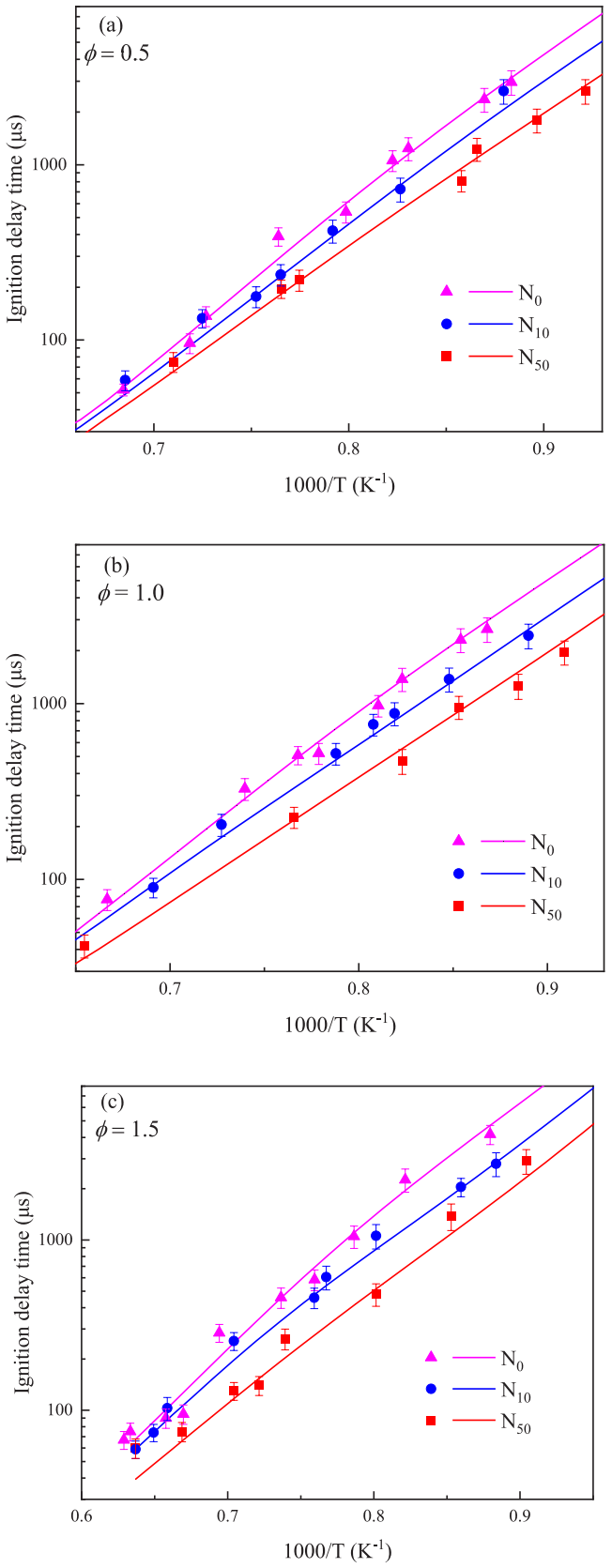

Figure 7. Ignition delay of $C_2H_5OH/NO_2/O_2/Ar$ mixtures with different NO_2 contents: (a) ϕ = 0.5, (b) ϕ = 1.0, and (c) ϕ = 1.5.

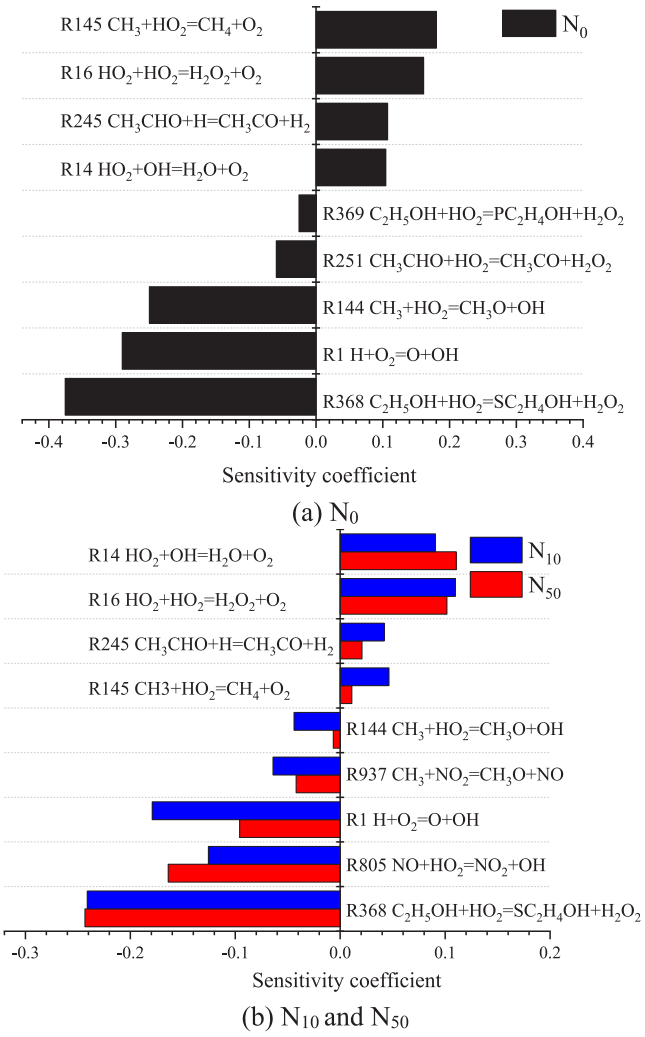

Figure 8. Sensitivity coefficient of ethanol under (a) N_0 and (b) N_{10} and N_{50} mixtures (ϕ = 1.0; T = 1150 K; P = 0.20 MPa).

interconversion between R805 and NO_2. In the N_{50} mixture, the proportion of the intermediate product CH_2CHO that directly reacted with NO_2 accounted for 81.06% of its total consumption. Overall, from the reaction pathway analysis, NO_2 reacts less directly with ethanol and its intermediates and mainly increases the number of OH generated in the radical pool by influencing the formation and interaction between small-molecule radicals to influence the ignition process of ethanol fuel.

3.3.3. Radical Mole Fraction. Figure 10 shows the variation in the molar fraction of key small-molecule species as a function of fuel consumption for the conditions at an equivalence ratio of 1 and T = 1150 K. As seen by the Figure 10a, the formed OH radicals increased significantly as the NO_2 proportion increased by consuming the same proportion of ethanol. It is noteworthy that the increment in OH radicals for the N_{10} mixture was not significant compared to the N_0 mixture, which further explains the small shortening rate of the ignition delay time for the N_{10} mixture relative to the N_0 mixture. As shown in the Figure 10b, with the addition of NO_2, the production of H radicals increased with increasing ethanol consumption. And the results show that the addition of NO_2 can significantly increase the peak value of both the OH and H radical mole fractions. The concentrations of these radicals increase with increasing NO_2 ratio, resulting in an enhancing reactivity to the system and decreasing ignition delay times.

https://doi.org/10.1021/acsomega.2c07167
ACS Omega 2023, 8, 8377−8387

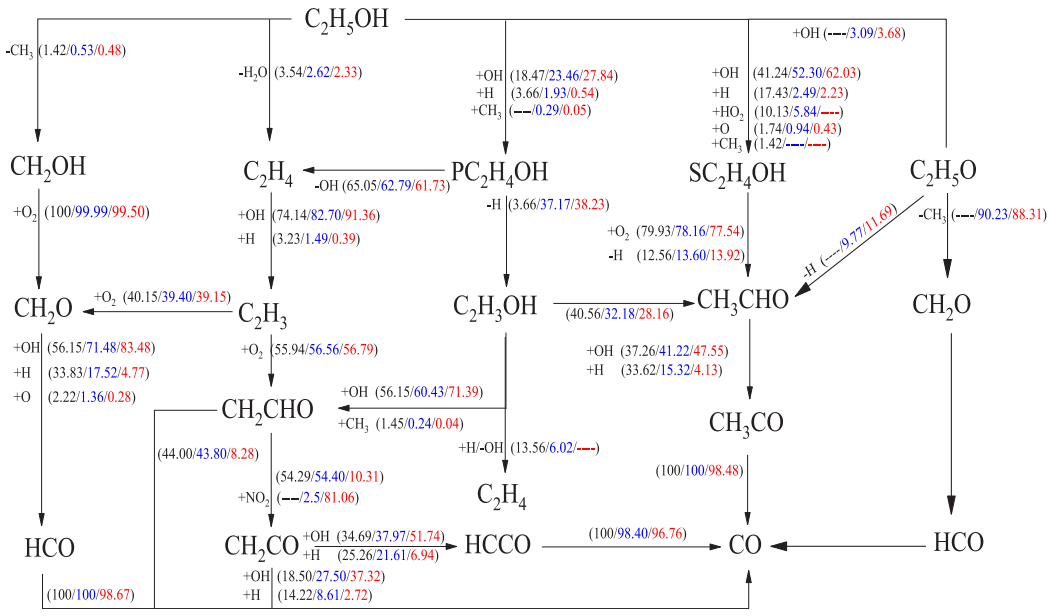

Figure 9. Reaction path of ethanol under different NO_2 contents (ϕ = 1.0; T = 1150 K; P = 0.20 MPa).

The production of HO_2 radicals as shown in Figure 10c decreases with increasing NO_2 proportion, which is due to the consumption of HO_2 radicals produced through reaction R805. In Figure 10d, the amount of H_2O_2 produced also decreased with an increase in NO_2 content. This is because H_2O_2 is primarily formed through the reaction of ethanol with HO_2 in R368. While reaction R805 competes with reaction R368, as the NO_2 proportion increases, more HO_2 is available for reaction R805. It can also be seen from Figure 10e,f that the production of stable small-molecule products through chain termination reactions, such as H_2 and CH_4, decrease with increasing NO_2. In conclusion, with the addition of NO_2, there was an increase in the production of species that contributed to ignition, whereas the production of species that inhibited ignition decreased.

3.3.4. Important Elementary Reactions. As described above, the H atom abstraction reaction initiating OH radicals consumes the vast majority of ethanol. The generation of other radicals such as H and HO_2 in the system is inhibited due to the effect of NO_X, and these small-molecule radicals were consumed via the reactions, while the active OH radicals are produced. Therefore, a production analysis was performed for the main consumption reactions of H and HO_2. Figure 11 shows that the rates of H and HO_2 radicals production in the mixtures of N_0, N_{10}, and N_{50} with time at P = 0.20 MPa, T = 1150 K, and stoichiometric condition. The horizontal coordinate in the figure is the normalized ignition delay time, which is the ratio of the reaction time to the ignition delay time to observe the variation of OH radical production before the ignition moment. The starting point of the horizontal coordinate in Figure 11 is 0.7 because of the low yield of radicals in the system at the early stage of ignition. The negative yield is shown in Figure 11a; for the N_0 and N_{10} mixtures, the reaction R1 consumes many H radicals to generate OH radicals before the ignition moment. In contrast, for the N_{50} mixture, the H radicals consumption rate near the ignition moment is significantly smaller than that of the N_0 and N_{10} mixtures, which is in accordance with the results of the sensitivity analysis regarding the different sensitivity coefficients of R1 for mixtures with different NO_2 proportions. The largest effect on HO_2 consumption is for the NO_X-related reaction R805 ($NO + HO_2 \Leftrightarrow NO_2 + OH$). The rate of HO_2 consumption in the N_{50} mixture is significantly faster than that in the N_{10} mixture, and a large number of OH radicals are generated while consuming HO_2. NO is mainly generated through the reaction of R938 ($CH_3 + NO_2 \Leftrightarrow CH_3O + NO$) and R808 ($NO_2 + H \Leftrightarrow NO + OH$). It is obvious in Figure 11b that the rate of HO_2 consumption in the N_{50} mixture is significantly faster than that in the N_{10} mixture, and a large number of OH radicals are generated while consuming HO_2. With the NO molar fraction decreasing, the slope of the HO_2 yield curve consumed through R805 increases as the ignition moment is approached, and the rate of OH radical production is faster, which is one of the main reasons for the shorter ignition delay time of the N_{50} mixture compared to the N_{10} mixture. The concentration of NO experiences a peak before ignition and then gradually decrease, leading to a decrease in HO_2 consumed by R805.

4. CONCLUSIONS

In this study, to expand the database of alcohol/NO_X interactions and to develop a detailed kinetic mechanism, the ignition delay time of ethanol/NO_2/O_2/Ar mixtures was measured behind reflected shock waves at a pressure of 0.20 MPa, temperature range of 1050−1650 K, and equivalence ratios of 0.5, 1.0, and 1.5, with ethanol/NO_2 blending ratios of 100/0, 90/10, and 50/50. Sensitivity analysis, reaction path analysis, and fundamental reaction analysis for mixtures with stoichiometric ratios were carried out using the established mechanism. The main conclusions are summarized as follows:

(1) The results show that the effect of NO_2 on ethanol is related to temperature and equivalence ratio and is particularly significant at decreasing temperature and increasing equivalence ratio conditions. The promotional effect of NO_2 was more significant for mixtures with higher NO_2 concentrations.

(2) The promotion of NO_2 occurs mainly through an increase in the rate and concentration of the free radical

https://doi.org/10.1021/acsomega.2c07167
ACS Omega 2023, 8, 8377−8387

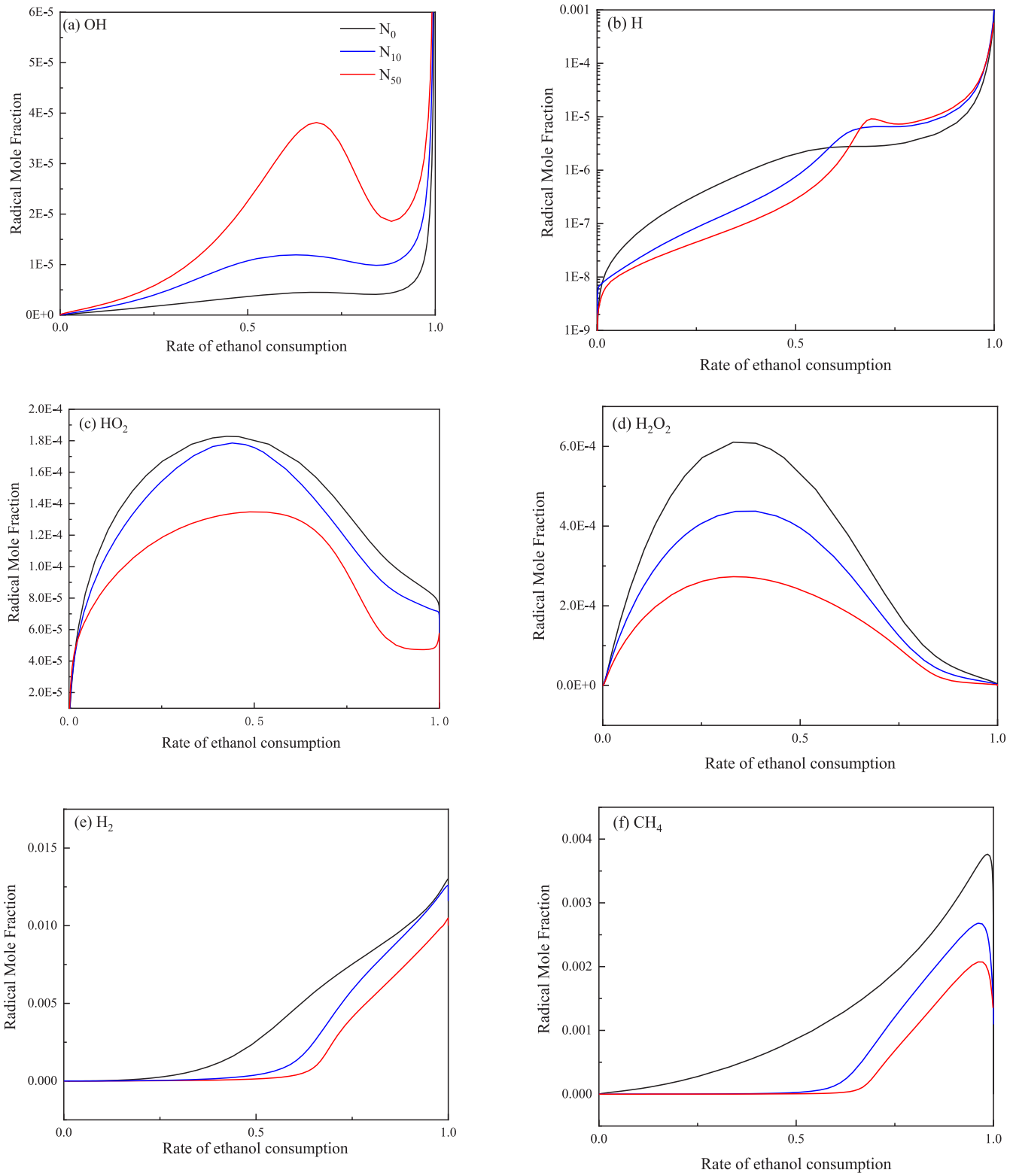

Figure 10. Changes of small molecules' species with fuel consumption ratio during ethanol ignition: (a) OH, (b) H, (c) HO_2, (d) H_2O_2, (e) H_2, and (f) CH_4.

pool, especially the OH radical pool, and the relevant reaction branch ratio of NO_2 expands significantly. Compared with pure ethanol, the formation of OH radicals occurs mainly through R805 ($NO + HO_2 \Leftrightarrow NO_2 + OH$) rather than R1($H + O_2 \Leftrightarrow O + OH$).

(3) With the addition of NO_2, because of its high reactivity, some reactive intermediate species are generated during the reaction, leading to further reactions of relatively unreactive species. The CH_3 radicals interact with NO_2 through the reaction R938 ($CH_3 + NO_2 \Leftrightarrow CH_3O + NO$), and the CH_2O radicals interact with NO_2 through

https://doi.org/10.1021/acsomega.2c07167
ACS Omega 2023, 8, 8377−8387

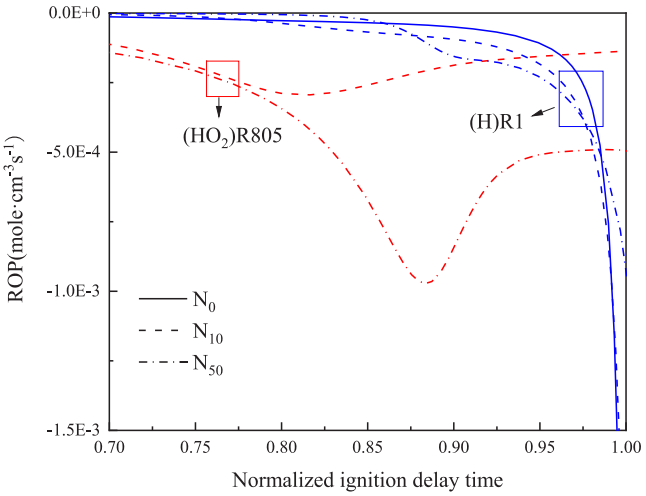

Figure 11. Rate of production of HO_2 and H radicals (ϕ = 1.0; T = 1150 K; P = 0.20 MPa).

reaction R911 ($CH_2O + NO_2 \Leftrightarrow HONO + HCO$) to form more reactive radicals, thus further enhancing the reactivity.

(4) The promotion of ethanol ignition by NO_2 is well-related to the interconversion between NO and NO_2, which leads to the fuel consumption and converts HO_2 radicals to chain excited OH radicals. Highly reactive H atoms and OH radicals significantly interfere with the initial reaction, thus enhancing the reactivity of the ethanol mixture.

■ ASSOCIATED CONTENT

Supporting Information

The Supporting Information is available free of charge at https://pubs.acs.org/doi/10.1021/acsomega.2c07167.

Updated mechanism files (ZIP)

All experimental data of ignition delay times in this work (PDF)

■ AUTHOR INFORMATION

Corresponding Author

Zhihao Ma − *School of Vehicle and Traffic Engineering, Henan University of Science and Technology, Luoyang, Henan 471003, People's Republic of China*; Phone: +86 18625983908; Email: mazhihao@haust.edu.cn

Authors

Yifan Jin − *School of Vehicle and Traffic Engineering, Henan University of Science and Technology, Luoyang, Henan 471003, People's Republic of China*; orcid.org/0000-0002-5304-4459

Xin Wang − *School of Vehicle and Traffic Engineering, Henan University of Science and Technology, Luoyang, Henan 471003, People's Republic of China*; orcid.org/0000-0003-2426-0459

Fangjie Liu − *School of Vehicle and Traffic Engineering, Henan University of Science and Technology, Luoyang, Henan 471003, People's Republic of China*; orcid.org/0000-0002-4514-146X

Xin Li − *School of Vehicle and Traffic Engineering, Henan University of Science and Technology, Luoyang, Henan 471003, People's Republic of China*

Xianglin Chu − *School of Vehicle and Traffic Engineering, Henan University of Science and Technology, Luoyang, Henan 471003, People's Republic of China*

Complete contact information is available at: https://pubs.acs.org/10.1021/acsomega.2c07167

Notes

The authors declare no competing financial interest.

■ ACKNOWLEDGMENTS

The authors acknowledge financial support from the National Natural Science Foundation of China (Grant No. 51906061) and the Science and Technology Department of Henan Province (Grant No. 222102320091).

■ REFERENCES

(1) Wang, M.; Saricks, C.; Santini, D. *Effects of fuel ethanol use on fuel-cycle energy and greenhouse gas emissions*, Report ANL/ESD-38; Center for Transportation Research, Argonne National Laboratory, U.S. Department of Energy: Chicago, IL, USA, 1999. DOI: 10.2172/4742.

(2) Park, C.; Choi, Y.; Kim, C.; Oh, S.; Lim, G.; Moriyoshi, Y. Performance and exhaust emission characteristics of a spark ignition engine using ethanol and ethanol-reformed gas. *Fuel* **2010**, *89* (8), 2118−2125.

(3) García, C. A.; Manzini, F.; Islas, J. Air emissions scenarios from ethanol as a gasoline oxygenate in Mexico City Metropolitan Area. *Renewable Sustainable Energy Rev.* **2010**, *14* (9), 3032−3040.

(4) Hori, M. Nitrogen dioxide formation by the mixing of hot combustion gas with cold air. *Symp. (Int.) Combust.* **1989**, *22*, 1175−1181.

(5) Rößler, M.; Koch, T.; Janzer, C.; Olzmann, M. Mechanisms of the NO_2 Formation in Diesel Engines. *MTZ Worldwide* **2017**, *78* (7−8), 70−75.

(6) Kimbrough, S.; Owen, R. C.; Snyder, M.; Richmond-Bryant, J. NO to NO(2) Conversion Rate Analysis and Implications for Dispersion Model Chemistry Methods using Las Vegas, Nevada Near-Road Field Measurements. *Atmos. Environ.* **2017**, *165*, 23−34.

(7) Contino, F.; Foucher, F.; Dagaut, P.; Lucchini, T.; D'Errico, G.; Mounaïm-Rousselle, C. Experimental and numerical analysis of nitric oxide effect on the ignition of iso-octane in a single cylinder HCCI engine. *Combust. Flame* **2013**, *160* (8), 1476−1483.

(8) Machrafi, H.; Guibert, P.; Cavadias, S. HCCI Engine Modeling and Experimental Investigations − Part 2: The Composition of a NO-PRF Interaction Mechanism and the Influence of NO in EGR on Auto-Ignition. *Combust. Sci. Technol.* **2008**, *180* (7), 1245−1262.

(9) Zangooee, M.; Modarres, R. A comprehensive numerical study of the ethanol blended fuel effect on the performance and pollutant emissions in spark-ignition engine. *Thermal Science* **2014**, *18* (1), 29−38.

(10) Maurya, R. K.; Agarwal, A. K. Experimental investigations of performance, combustion and emission characteristics of ethanol and methanol fueled HCCI engine. *Fuel Process. Technol.* **2014**, *126*, 30−48.

(11) Cancino, L. R.; Fikri, M.; Oliveira, A. A. M.; Schulz, C. Ignition delay times of ethanol-containing multi-component gasoline surrogates: Shock-tube experiments and detailed modeling. *Fuel* **2011**, *90* (3), 1238−1244.

(12) Shin, K.-S.; Park, K.-S.; Gwon, E.-S. Shock Tube and Modeling Study of Ethanol Ignition. *J. Korean Chem. Soc.* **2004**, *48* (1), 12−16.

(13) Zhang, Y.; El-Merhubi, H.; Lefort, B.; Le Moyne, L.; Curran, H. J.; Kéromnès, A. Probing the low-temperature chemistry of ethanol via the addition of dimethyl ether. *Combust. Flame* **2018**, *190*, 74−86.

(14) Barraza-Botet, C. L.; Wagnon, S. W.; Wooldridge, M. S. Combustion Chemistry of Ethanol: Ignition and Speciation Studies in a Rapid Compression Facility. *J. Phys. Chem. A* **2016**, *120* (38), 7408−7418.

(15) Mittal, G.; Burke, S. M.; Davies, V. A.; Parajuli, B.; Metcalfe, W. K.; Curran, H. J. Autoignition of ethanol in a rapid compression machine. *Combust. Flame* **2014**, *161* (5), 1164−1171.
(16) Herrmann, F.; Jochim, B.; Oßwald, P.; Cai, L.; Pitsch, H.; Kohse-Höinghaus, K. Experimental and numerical low-temperature oxidation study of ethanol and dimethyl ether. *Combust. Flame* **2014**, *161* (2), 384−397.
(17) Dagaut, P.; Togbé, C. Experimental and Modeling Study of the Kinetics of Oxidation of Ethanol−Gasoline Surrogate Mixtures (E85 Surrogate) in a Jet-Stirred Reactor. *Energy Fuels* **2008**, *22* (5), 3499−3505.
(18) Laich, A. R.; Ninnemann, E.; Neupane, S.; Rahman, R.; Barak, S.; Pitz, W. J.; Goldsborough, S. S.; Vasu, S. S. High-pressure shock tube study of ethanol oxidation: Ignition delay time and CO time-history measurements. *Combust. Flame* **2020**, *212*, 486−499.
(19) Nativel, D.; Niegemann, P.; Herzler, J.; Fikri, M.; Schulz, C. Ethanol ignition in a high-pressure shock tube: Ignition delay time and high-repetition-rate imaging measurements. *Proc. Combust. Inst.* **2021**, *38* (1), 901−909.
(20) Cheng, S.; Kang, D.; Goldsborough, S. S.; Saggese, C.; Wagnon, S. W.; Pitz, W. J. Experimental and modeling study of C2−C4 alcohol autoignition at intermediate temperature conditions. *Proc. Combust. Inst.* **2021**, *38* (1), 709−717.
(21) Sahu, A. B.; Mohamed, A. A. E.-S.; Panigrahy, S.; Saggese, C.; Patel, V.; Bourque, G.; Pitz, W. J.; Curran, H. J. An experimental and kinetic modeling study of NO_X sensitization on methane autoignition and oxidation. *Combust. Flame* **2022**, *238*, 111746.
(22) Mohamed, A. A. E.-S.; Panigrahy, S.; Sahu, A. B.; Bourque, G.; Curran, H. The effect of the addition of nitrogen oxides on the oxidation of ethane: An experimental and modelling study. *Combust. Flame* **2022**, *241*, 112058.
(23) Deng, F.; Zhang, Y.; Sun, W.; Huang, W.; Zhao, Q.; Qin, X.; Yang, F.; Huang, Z. Towards a kinetic understanding of the NO_X sensitization effect on unsaturation hydrocarbons: A case study of ethylene/nitrogen dioxide mixtures. *Proc. Combust. Inst.* **2019**, *37* (1), 719−726.
(24) Wu, H.; Sun, W.; Huang, Z.; Zhang, Y. Biphasic sensitization effect of NO_2 on n-C_4H_{10} auto-ignition. *Combust. Flame* **2022**, *237*, 111844.
(25) Shi, L.; Chen, D.; Zheng, Z.; Xu, P.; Wang, R.; Zhang, C. An experimental and kinetic study the effect of nitrogen dioxide addition on autoignition of n-heptane. *Combust. Flame* **2021**, *232*, 111540.
(26) Ye, W.; Shi, J. C.; Zhang, R. T.; Wu, X. J.; Zhang, X.; Qi, M. L.; Luo, S. N. Experimental and Kinetic Modeling Study of CH3OCH3Ignition Sensitized by NO_2. *Energy Fuels* **2016**, *30* (12), 10900−10908.
(27) Chen, Z.; Zhang, P.; Yang, Y.; Brear, M. J.; He, X.; Wang, Z. Impact of nitric oxide (NO) on n-heptane autoignition in a rapid compression machine. *Combust. Flame* **2017**, *186*, 94−104.
(28) Gersen, S.; Mokhov, A. V.; Darmeveil, J. H.; Levinsky, H. B.; Glarborg, P. Ignition-promoting effect of NO_2 on methane, ethane and methane/ethane mixtures in a rapid compression machine. *Proc. Combust. Inst.* **2011**, *33* (1), 433−440.
(29) Herzler, J.; Naumann, C. Shock Tube Study of the Influence of NO_X on the Ignition Delay Times of Natural Gas at High Pressure. *Combust. Sci. Technol.* **2012**, *184* (10−11), 1635−1650.
(30) Yang, C.; Li, Y.; Wang, W.; Cheng, X. Shock tube experimental studies on the ignition delay of n-heptane/ethanol fuel blends with acetaldehyde (CH_3CHO) and oxynitride(NO/NO_2) additives. *Int. J. Engine Res.* **2022**, No. 14680874221085635.
(31) Alzueta, M. U.; Hernández, J. M. Ethanol Oxidation and Its Interaction with Nitric Oxide. *Energy Fuels* **2002**, *16* (1), 166−171.
(32) Morley, C. *Gaseq*, Version 0.76; 2005. http://www.gaseq.co.uk.
(33) Petersen, E. L.; Rickard, M. J. A.; Crofton, M. W.; Abbey, E. D.; Traum, M. J.; Kalitan, D. M. A facility for gas- and condensed-phase measurements behind shock waves. *Meas. Sci. Technol.* **2005**, *16* (9), 1716−1729.
(34) *CHMEKIN-PRO*; Reaction Design: San Diego, CA, USA, 2018. https://www.Ansys.com/.
(35) Ranzi, E.; Frassoldati, A.; Grana, R.; Cuoci, A.; Faravelli, T.; Kelley, A. P.; Law, C. K. Hierarchical and comparative kinetic modeling of laminar flame speeds of hydrocarbon and oxygenated fuels. *Prog. Energy Combust. Sci.* **2012**, *38* (4), 468−501.
(36) Mathieu, O.; Pinzón, L. T.; Atherley, T. M.; Mulvihill, C. R.; Schoel, I.; Petersen, E. L. Experimental study of ethanol oxidation behind reflected shock waves: Ignition delay time and H_2O laser-absorption measurements. *Combust. Flame* **2019**, *208*, 313−326.
(37) Metcalfe, W. K.; Burke, S. M.; Ahmed, S. S.; Curran, H. J. A Hierarchical and Comparative Kinetic Modeling Study of C1 − C2 Hydrocarbon and Oxygenated Fuels. *Int. J. Chem. Kinet.* **2013**, *45* (10), 638−675.
(38) Sarathy, S. M.; Oßwald, P.; Hansen, N.; Kohse-Höinghaus, K. Alcohol combustion chemistry. *Prog. Energy Combust. Sci.* **2014**, *44*, 40−102.
(39) Zhang, Y.; Mathieu, O.; Petersen, E. L.; Bourque, G.; Curran, H. J. Assessing the predictions of a NO_X kinetic mechanism on recent hydrogen and syngas experimental data. *Combust. Flame* **2017**, *182*, 122−141.
(40) Shrestha, K. P.; Seidel, L.; Zeuch, T.; Mauss, F. Kinetic Modeling of NO_X Formation and Consumption during Methanol and Ethanol Oxidation. *Combust. Sci. Technol.* **2019**, *191* (9), 1627−1659.
(41) Glarborg, P.; Miller, J. A.; Ruscic, B.; Klippenstein, S. J. Modeling nitrogen chemistry in combustion. *Prog. Energy Combust. Sci.* **2018**, *67*, 31−68.
(42) Bugler, J.; Somers, K. P.; Simmie, J. M.; Guthe, F.; Curran, H. J. Modeling Nitrogen Species as Pollutants: Thermochemical Influences. *J. Phys. Chem. A* **2016**, *120* (36), 7192−7197.
(43) Dean, A. M.; Bozzelli, J. W. Combustion chemistry of nitrogen. In *Gas-phase combustion chemistry*, 2nd ed; Gardiner, W. C., Ed.; Academic Press, Springer: New York, NY, 2000; pp 125−341. DOI: 10.1007/978-1-4612-1310-9_2.
(44) Baulch, D. L.; Bowman, C. T.; Cobos, C. J.; Cox, R. A.; Just, T.; Kerr, J. A.; Pilling, M. J.; Stocker, D.; Troe, J.; Tsang, W.; et al. Evaluated Kinetic Data for Combustion Modeling: Supplement II. *J. Phys. Chem. Ref. Data* **2005**, *34* (3), 757−1397.
(45) Lopez, J. G.; Rasmussen, C. L.; Alzueta, M. U.; Gao, Y.; Marshall, P.; Glarborg, P. Experimental and kinetic modeling study of C2H4 oxidation at high pressure. *Proc. Combust. Inst.* **2009**, *32* (1), 367−375.
(46) Klippenstein, S. J.; Pfeifle, M.; Jasper, A. W.; Glarborg, P. Theory and modeling of relevance to prompt-NO formation at high pressure. *Combust. Flame* **2018**, *195*, 3−17.

NOTE ADDED AFTER ASAP PUBLICATION

After this paper was published ASAP February 22, 2023, a spelling error in the title was corrected. The corrected version was published online March 7, 2023.

https://doi.org/10.1021/acsomega.2c07167
ACS Omega 2023, 8, 8377−8387